Ferromagnetic forces acting on the EU-DEMO divertor

G. Di Mambro[a,b], A. Maffucci[a,b], G. Mazzone[c], G. Rubinacci [a,d], S. Ventre[a,b], F. Villone[a,d] , J.H. You[e]

[a] CREATE Consortium, Via Claudio 21, 80125 Naples (Italy)

[b] DIEI, Dept. of Electrical and Information Engineering, DIEI, University of Cassino and Southern Lazio, Via G. Di Biasio 43, 03043, Cassino (FR), Italy

[c] ENEA, Dept. of Fusion and Technology for Nuclear Safety and Security, Via Fermi 45, 00044 Frascati (RM), Italy

[d] DIETI, Dept. of Electrical Engineering and Information Technology, University of Naples Federico II, Via Claudio 21, 80125 Naples (Italy)

[e] Max Planck Institute for Plasma Physics, Boltzmann str. 2, 85748 Garching, Germany

Corresponding author: Gennaro Di Mambro, mail to: gennaro.dimambro@unicas.it

---

ABSTRACT

This paper presents an analysis of the mechanical loads produced by the ferromagnetic effects in the divertor of the European DEMO (EU-DEMO) reactor. The exact assessment of this force is an important prerequisite for a reliable structural design, for instance for a correct choice of the fixing supports. To this end, a 3D magnetostatic model has been built with a simplified geometry corresponding to a 22.5° angular sector of the tokamak, exploiting the toroidal symmetry and imposing periodic boundary conditions. The problem has been solved by using CARIDDI code, that implements an integral formulation and provides a significant simplification of the numerical model, since the mesh can be limited to the magnetic materials only. In our case, the main components of the model (divertor and breeding blankets) are made of a ferromagnetic material, namely, EUROFER97 steel. In presence of external static magnetic fields, these components would behave like an "electromagnet" being subjected to forces. The model considers all the sources of such magnetizing fields, namely: (i) the external toroidal field produced by the currents circulating in the external toroidal field coils, (ii) the internal field induced by the toroidal plasma current. Expected static field in the considered components ranges from 3.4 T to 8.6 T. Forces and torques have been evaluated by Kelvin method, starting from the known external magnetic fields and the computed magnetization in the ferromagnetic regions. The contribution of the static magnetic field associated to the equilibrium plasma current has been shown to be negligible.

KEYWORDS

European DEMO, Divertor, Electromagnetic loads, Ferromagnetism, Kelvin method.

---

1. INTRODUCTION

Low activation ferritic/martensitic steels such as RAFM [1] and EUROFER97 [2] are attractive materials proposed for large structural elements of nuclear fusion reactors, such as for instance blankets [3]. Indeed, the low activation characteristic reduces the issues associated to radioactive waste produced by neutron irradiation, so improving the operational availability and simplifying the decommissioning process.

The presence of ferromagnetic materials has an impact on plasma equilibrium and mechanical stability. Indeed, the impact of the presence of ferromagnetic materials on plasma equilibrium is known (e.g., [4]-[7]), and can be conveniently exploited, for instance with a suitable use of ferromagnetic inserts to reduce toroidal field ripples [8]. In general, ferromagnetic effects must be included in plasma equilibrium analysis as they can be sources of destabilization [4]-[7].

The mechanical consequences of the use of ferromagnetic steels are instead associated to the forces

that arise from the magnetization of these materials. These forces must be properly accounted together with those related to eddy currents and halo currents, to accurately define the electromagnetic (EM) loads that the structural elements are required to withstand [9]-[13].

In this paper, we analyse the mechanical loads produced by the ferromagnetic effects on the divertor of the European DEMO (EU-DEMO) reactor [14]. The Pre-Conceptual Design activities to develop the EU-DEMO divertor has been concluded [15], with the definition of the main characteristics of the systems, starting from the size of the machine itself (a major radius of about 9 m and a fusion power of about 2000 MW). During such a phase, the mechanical effect of the ferromagnetic forces has been highlighted, for instance in estimating the pre-compression force acting on the breeding blanket structural materials, in view of a correct design of the blanket attachments [16]-[17].

Reviewer comment to be addressed: Please rephrase. It is not clear if the pre-compression forces are applied preventively in the blanket for withstanding the pulling forces acting on the blanket segments during normal operation. In case the forces the blanket withstand during normal operation are compressive, they cannot be defined as pre-compressive. The "pre" indicates that a preventive action is put in place for counterbalancing an undesired effect.

Following on this, in this paper we focus the attention on the ferromagnetic interaction between divertor cassettes and blankets in EU-DEMO, being both made of EUROFER 97. These interactions are expressed by forces and torques acting on these structures, as a consequence of their magnetization and of the spatial variation of the toroidal magnetic field. The model proposed here in Section 2, describes this problem in a static limit, assuming a 22.5° sector of DEMO machine, including all the ferromagnetic components. The exciting sources of the model are given by the external toroidal field coils or induced by the internal field induced by the toroidal plasma currents. The integral formulation implemented in CARIDDI code [18] is used, that allows lowering the computational cost of the analysis since it is based on a formulation for which only the conducting and magnetic regions must be meshed. Section 3 reports the analysis results and related discussion.

2. EM Model of the Divertor

2.1 Geometry and materials

By exploiting the symmetries of the DEMO machine, the whole structure can be seen as the result of 16 toroidal rotations of a sector of 22.5°. The 3D analysis is then performed on such a sector, imposing periodicity conditions on the magnetization $\boldsymbol{M}$ at the boundaries:

$$\boldsymbol{M}(r,z,j) = \boldsymbol{M}(r,z,j+2k/16) \text{ for } k=1..16. \quad (1)$$

The CAD model of a single divertor module is reported in Fig.1, and refers to the version at the end of the Pre-Conceptual Design phase. ITER global reference system is adopted, with x-, y- and z- axes corresponding to the radial, toroidal and vertical directions, respectively.

The model only includes the ferromagnetic elements (divertor cassettes and blankets) and the excitations. This is a direct consequence of the adopted EM formulation, as outlined later. Three divertor modules and three blanket modules fall in the considered sector, as shown in Fig.3.

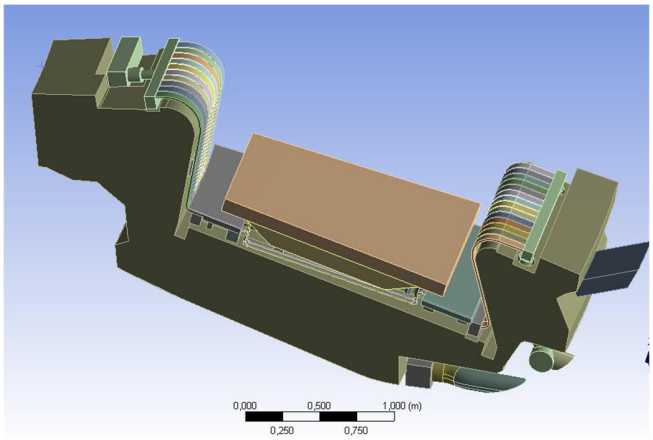

Fig. 2. CAD model of a single divertor module.

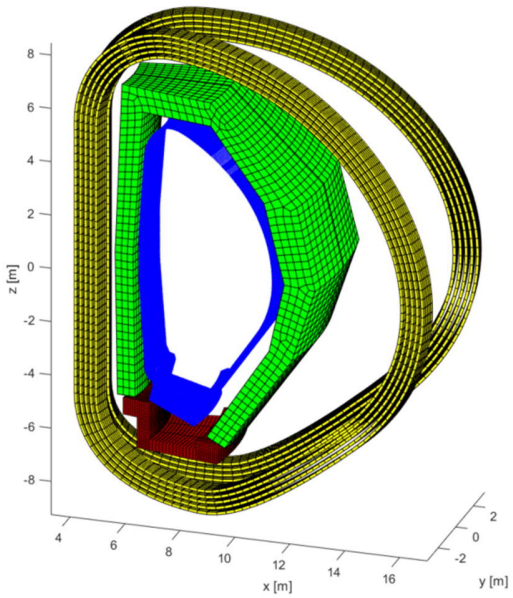

Fig. 3. The analyzed 22.5° sector of DEMO in-vessel assembly, including the divertors (in red), blankets (in green), the toroidal field coils (in yellow) and the layer with the equivalent sources associated to plasma currents (in blue). (b) the considered ferromagnetic components

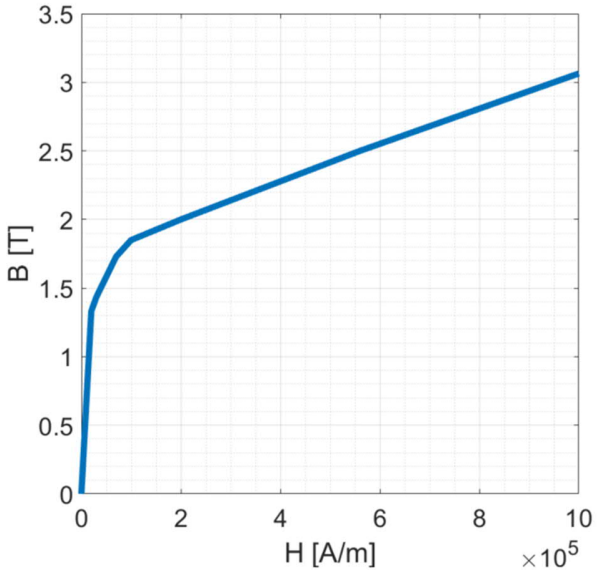

Fig. 4. B-H magnetization curve of the Eurofer97 steel [2].

Table 1. EUROFER97 properties [2], [19]

Components	Material	Resistivity (Ωm)	Relative Permeability
Blanket, divertor cassettes	EUROFER97	$8.54 \cdot 10^{-7}$	39 – 53

The resistivity and permeability of the materials are listed in Table 1, taken from [2], [19]. Note that the permeability values refer to the linear tract of the B-H curve in Fig.4, derived from the data in [2]. Note that, as pointed out in [20], this characteristic can be affected by actual temperature values and neutron irradiation levels typical of operating conditions.

Finally, we underline that the CAD models describing the ferromagnetic elements have been strongly simplified (for instance, with respect to the model in Fig. 2), but retaining approximatively the same volume of the original model. Specifically, the volume of each of the three cassettes is equal to 2.3 m^3, whereas that of each of the two blanket modules is 42 m^3. Furthermore, the ratio p between ferromagnetic/no ferromagnetic volumes is equal to 38.3% in the cassettes and to 8.3% in the blankets. Therefore, the EUROFER volume of three divertors is equal to 2.64 m^3 whereas that of the two blankets is equal to 6.80 m^3.

Therefore, the accuracy of the results can be estimated within such a range, since all the other steps are associated to a higher accuracy (e.g., mesh refinement, numerical solution convergence, etc..).

2.2 Excitation sources

The excitation sources of the model imposes in the considered sector a value of the static field that corresponds to the equilibrium scenario defined in [21]. Specifically, the desired static field configuration is created by imposing a total current of 32.6MA flowing through the toroidal field coils (TFCs), and by adding the contribution coming from the plasma current at equilibrium. The latter contribution is imposed by considering equivalent currents flowing through a high number of toroidally directed filaments, see blue layer in Fig.3. The identification of these equivalent currents has been obtained through plasma simulations carried out with the CarMa0NL code [22]. The total current resulting from this evaluation is equal to 19.07 MA. As it will be shown in Section 3, the contribution to the loads coming from this term is a correction to the main one coming from the TF coils. Other possible contributions, coming from

axisymmetric sources (for instance, Poloidal Field coils) are found to be negligible.

2.3 Electromagnetic model and load evaluation

As pointed out, the analysis has been performed by using CARIDDI code [18], for two main reasons. This code allows a great simplification of the meshing, since it requires the discretization of the metallic parts only (magnetic or conducting). In addition, it solves non-linear problems by means of a Picard-Banach procedure, whose convergence is theoretically guaranteed for a large class of magnetic constitutive equations, including the *B-H* relation of EUROFER analysed in this paper.

By using such a tool, the problem is formulated in terms of the following a non-linear magneto-static volume integral equation in weak form:

$$\int_{V_M} \mathbf{W}_M \cdot \left[\mathcal{G}^{-1}(\mathbf{M}) - \mathcal{B}[\mathbf{M}] - \mathbf{B}_S \right] dV = 0, \forall \mathbf{W}_M \in \mathbf{L}^2(V_M) \qquad (2)$$

where $\mathbf{M}=\mathbf{G}(\mathbf{B})$ is the constitutive equation of the magnetic material in the domain V_M, and $\mathbf{B}_S$ is the vector potential given by the external sources, and the operator $\mathbf{B}$ is the magnetic flux density for an assigned magnetization $\mathbf{M}$, as defined through the Biot-Savart law. The magnetization $\boldsymbol{M}$ is in turns expressed as the linear combination of piecewise constant functions $\mathbf{P}_j$:

$$\mathbf{M}(\mathbf{r},t) = \sum_j M_j(t)\mathbf{P}_j(\mathbf{r}) \text{ in} V_M \qquad (3)$$

The solution is accomplished by means of a Picard-Banach iteration, and to this end, it is convenient to express the magnetization $\boldsymbol{M}$ in the following form:

$$\boldsymbol{M} = (\boldsymbol{B}/\mu_0 - \boldsymbol{H})p \qquad (4)$$

where $\boldsymbol{H} = \nu(B)\boldsymbol{B}$ is the magnetic field, $\nu(B)$ is the non-linear isotropic magnetic reluctivity of the magnetic material, and p is the ferromagnetic/no ferromagnetic volumes ratio.

Once the problem is solved, the forces $\mathbf{F}_k$ and torques $\mathbf{T}_k$ on the k-th element are evaluated using the Kelvin's Method, namely by calculating the following integrals:

$$\mathbf{F}_k = \int_{V_{Mk}} \mathbf{M} \cdot \nabla \mu_0 \mathbf{H}_{extk}\, dV \qquad (5)$$

$$\mathbf{T}_k = \int_{V_{Mk}} \mathbf{M}\, x\, \mu_0 \mathbf{H}_{extk}\, dV + \int_{V_{Mk}} r\, x\, \mathbf{F}_k\, dV \qquad (6)$$

Here, $\mathbf{H}_{ext}$ is the external magnetic field imposed by the external coils, and V_{Mk} is the volume of the considered ferromagnetic object. In addition to Kelvin formula, the loads have been all computed by means of the method of the equivalent magnetic charges, purely as cross-check.

A meshed divertor is shown in Fig. 5: an adaptive and conformal tetrahedrons meshing has been used, whose characteristic are reported in Table 2.

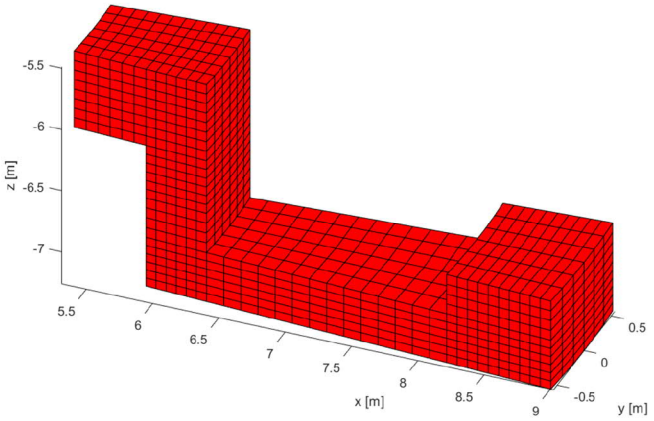

Fig. 5. View of the meshed divertor.

Table 2. Features of the blankets and the divertors meshes.

Component	Nodes	Elements
Divertor cassettes	9261	6768
Blanket modules	5852	3780

3. RESULTS AND DISCUSSION

3.1 Field maps

The spatial distribution of the magnetic flux density $\boldsymbol{B}$ in the considered regions is plotted in Fig.6,7 and 8. Specifically, Fig.6 shows the field imposed by the external sources in the regions of the divertor and of the blanket, assumed to be non-magnetic. The total field in the same regions, including the effect of magnetization, is instead shown in Fig.7. By comparing the two results, it is evident that the effect of the magnetization on the total $\boldsymbol{B}$ field is limited. To better highlight this point, Fig.8 reports the magnetic flux density associated to the induced magnetization. Note that the imposed field levels

are above the saturation limits for the EUROFER (see Fig.4).

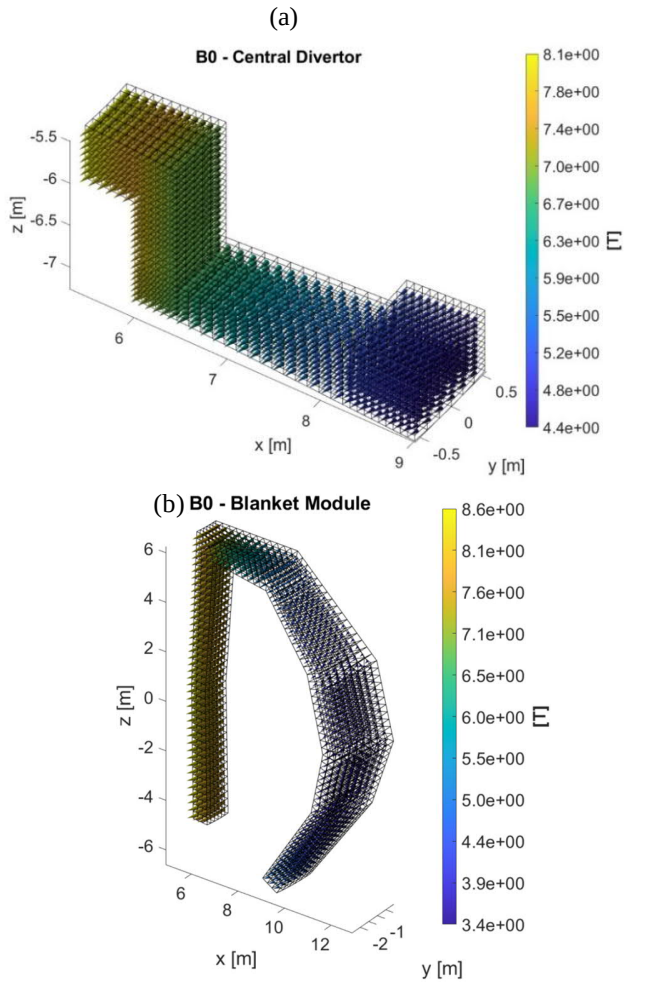

Fig. 6. Distribution of the magnetic flux density B in the ferromagnetic regions imposed by external excitations: (a) on the Central Divertor (b) on a blanket module.

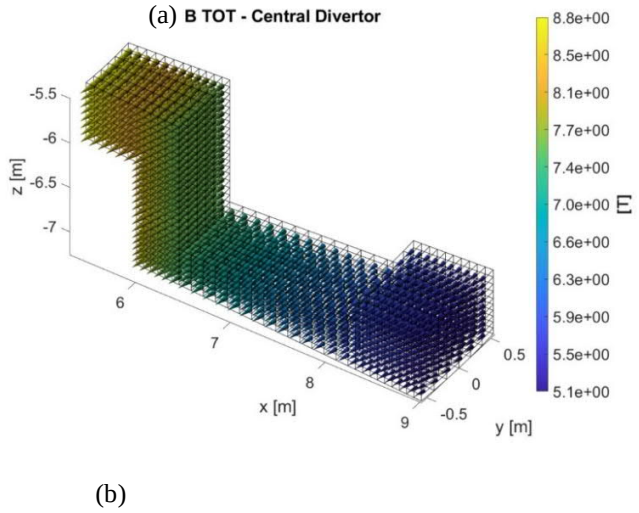

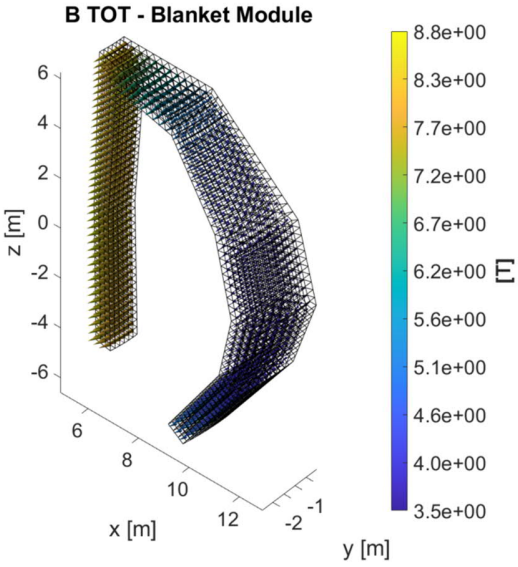

Fig. 7. Distribution of the total magnetic flux density: (a) on the Central Divertor (b) on a single Blanket module.

3.2 Evaluation of forces and moments

By using Kelvin's method (see (5) and (6)), the computed distributions of field and magnetization have been used to evaluate the resultant ferromagnetic forces and moments associated to each element of the model, as reported in Table 3. Note that the moments are computed with respect to the center of mass of each element.

Both for the divertors and for the blankets, the main component of the ferromagnetic resultant force is the radial one ($|F_x|_{max} = 1.25\ MN$ and $|F_x|_{max} = 3.27\ MN$), respectively, that results to be 1-2 orders of magnitude larger than the others. Considering the reference axes (See Fig.3), these radial forces are all directed towards the inner part of the machine.

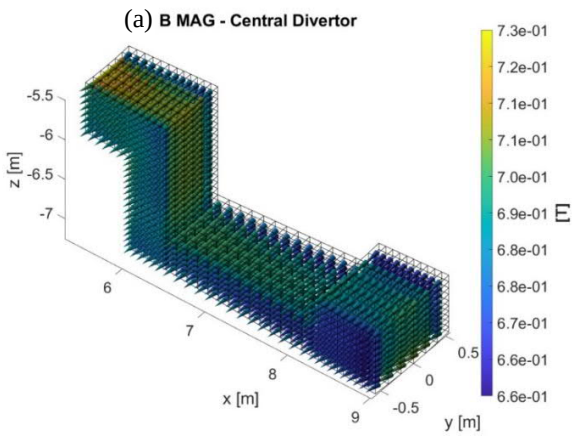

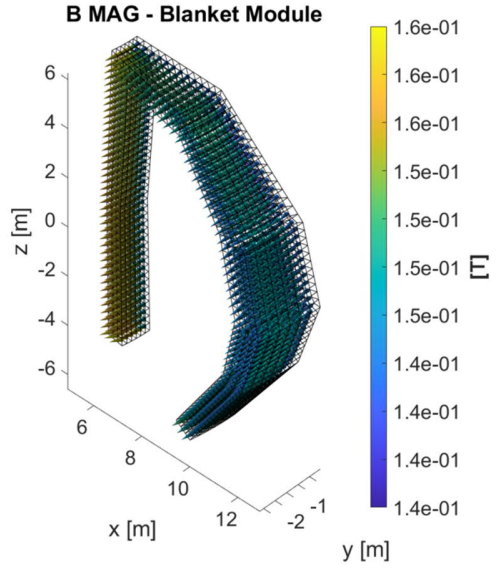

Fig. 8. Distribution of the magnetic flux density due to the magnetization of the ferromagnetic regions: (a) on the Central Divertor (b) on a single Blanket module.

As for the torques, in the divertors the main components are the toroidal ones ($|M_y|_{max} = 8.71\ MNm$), whereas in the blankets the toroidal and vertical ones are comparable ($|M_y|_{max} = 2.81\ MNm$, $|M_z|_{max} = 2.57\ MNm$).

To highlight the effect of the axisymmetric source (plasma current), the same analysis has been carried out by using the TF coils excitation only, and the results are summarized in Table 4. The variation on the peak values of forces and of moments is less than 5%, hence the contribution coming from such a source is negligible compared to the limits of the accuracy of the results of the proposed model.

Table 3. Computed values of the resultants of ferromagnetic forces and moments (total).

	Fx [MN]	Fy [MN]	Fz [MN]	Mx [MNm]	My [MNm	Mz [MNm]
Central Cassette	- 1.25	- 0.02	0.25	- 0.13	6.30	-0.14
External Cassette 1	- 1.20	0.11	- 0.09	0.67	8.60	2.00
External Cassette 2	- 1.19	- 0.08	- 0.12	- 0.50	8.71	-1.83
Blanket 1	-3.27	0.05	-0.02	0.05	-2.66	-2.57
Blanket 2	-3.27	-0.05	0.06	-0.04	-2.81	2.57

Table 4. Computed values of the resultants of ferromagnetic forces and moments (TF coils only).

	Fx [MN]	Fy [MN]	Fz [MN]	Mx [MNm]	My [MNm]	Mz [MNm]
Central Cassette	-1.25	0.00	0.24	0.01	6.41	0.01
External Cassette 1	-1.19	0.10	-0.13	0.58	8.78	1.93
External Cassette 2	-1.19	-0.10	-0.13	-0.57	8.78	-1.91
Blanket 1	-3.23	0.04	0.003	0.04	-2.81	-2.60
Blanket 2	-3.23	-0.04	0.003	-0.04	-2.81	2.60

As a final consideration, we may observe that the order of magnitude of these static loads is comparable to the EM loads coming from transient effects associated to the VDE event (eddy currents, halo currents), see [20]. Indeed, the peak values of forces and moments on the divertor assembly reported in [20] are about 1.3 MN and 3.2 MNm, hence these ferromagnetic loads play a non-negligible role in designing the mechanical structure.

4. CONCLUSIONS

The static ferromagnetic forces acting on the divertor cassettes and blanket modules of EU-DEMO machine have been here estimated, referred to 32.6MA TFC current scenario. The ferromagnetic steel EUROFER97 has been assumed for such elements. The adopted model corresponds to a 22.5° angular sector of the tokamak, where three divertor modules fall. The equilibrium field is imposed by assuming a non-axisymmetric source (TF coil currents) and an axisymmetric one (plasma current).

The peak values of the resultant force acting on divertor cassettes and blankets are attained by the radial component, and are equal to $1.25\ MN$ and $3.27\ MN$, respectively. The peak values of the resultant moments (computed with reference to the mass center of each module) are equal to $8.71\ MNm$ and $2.81\ MNm$, respectively.

The plasma current is demonstrated to have a negligible effect, since the above peak values change by less than 5% in presence or absence of such a source.

Work is in progress to check the effect of using ferromagnetic materials also for other divertor components such as those of the cooling system, so far designed to be non-magnetic.

ACKNOWLEDGEMENTS

This work has been carried out within the framework of the EUROfusion Consortium and has received funding from the Euratom research and training programme 2014-2018 and 2019-2020 under grant agreement No 633053.

The views and opinions expressed herein do not necessarily reflect those of the European Commission.

This work has been also supported in part by Italian MUR under PRIN grant 20177BZMAH".

REFERENCES

[1] A. Kohyama, A. Hishinuma, Y. Kohno, K. Shiba, and A. Sagara, "The development of ferritic steels for DEMO blanket, Fusion Eng. Des. 41 (1998), 1–6.

[2] K. Mergia, N. Boukos, Structural, thermal, electrical and magnetic properties of Eurofer 97 steel, Jour. Nuclear Materials, 373 (2008) 1-8.

[3] C. Cabet, F. Dalle, E. Gaganidze, J. Henry, H. Tanigawa, Ferritic-martensitic steels for fission and fusion applications, Jour. Nuclear Materials, 523 (2019) 510 - 537.

[4] V. D. Pustovitov, F. Villone, and JET-EFDA contributors, Effect of ferromagnetic structures on RWM growth rates: a cylindrical model and a verification on JET, Plasma Physics and Controlled Fusion, 52 (2010) 065010.

[5] G. Kurita, et al. Ferromagnetic and resistive wall effects on the beta limit in a tokamak, Nuclear fusion, 43 (2003) 949.

[6] Xiang Ji, et al., Investigation on the magnetic field distortion by ferromagnetism of the blanket for the helical fusion reactor, Fusion Engin. Design, 125 (2017) 631-634.

[7] O. P. Bardsleya, T. C. Hender, On the axisymmetric stability of tokamaks with ferromagnetic walls, Phys. Plasmas, 27 (2020) 102508.

[8] K. Tobita, T. Nakayama, S.V. Konovalov and M. Sato, Reduction of energetic particle loss by ferritic steel inserts in ITER, Plasma Phys. Control. Fusion 45 (2003) 133.

[9] R. Roccella, et al. Assessment of EM loads on the EU HCPB TBM during plasma disruption and normal operating scenario including the ferromagnetic effect, Fusion Eng. Design, 83 (2008) 1212-1216.

[10] M. Morimoto, et al. Electromagnetic analysis, structural integrity and progress on mechanical design of the ITER ferromagnetic insert. Fusion engineering and design, 84 (2009) 2118-2123.

[11] V.D. Pustovitov, G. Rubinacci and F. Villone, On the computation of the disruption forces in tokamaks, Nucl. Fusion, 57 (2017) 126038.

[12] H. Chen, Q. Xu, C. Jin and S. Wang, Model development and electromagnetic analysis of a vertical displacement event for the Chinese Fusion Engineering Test Reactor helium cooled solid blanket, Nucl. Fusion, 59 (2019) 056022.

[13] V.D. Pustovitov, Models and scalings for the disruption forces in tokamaks, Nucl. Fusion, 62 (2022) 026036.

[14] G. Federici et al, Overview of the DEMO staged design approach in Europe, Nucl. Fusion 59 (2019) 066013.

[15] J.H. You, et al., Divertor of the European DEMO: Engineering and technologies for power exhaust, Fusion Engin. Design, 175 (2022) 113010

[16] C. Bachmann et al., Overview over DEMO design integration challenges and their impact on component design concepts, Fusion Engin.eering and Design, 136 (2018) 87-95.

[17] C. Bachmann, L. Ciupinski, C. Gliss, T. Franke, T. Härtl, P. Marek, F. Maviglia, R. Mozzillo, R. Pielmeier, T. Schiller, P. Spaeh, T. Steinbacher, M. Stetka, T. Todd, C. Vorpahl, Containment structures and port configurations, Fusion Engineering and Design, 174 (2022) 112966.

[18] R. Albanese and G. Rubinacci, An integral formulation for. 3-D eddy current computation using edge elements, IEE Proceedings A, 135 (1988) 457-462.

[19] Material Property Handbook on EUROFER97, 2MT9X8_v1_0.

[20] G. Di Mambro, A. Maffucci, G. Mazzone, S. Ventre, F. Villone, J.H. You, Mechanical impact of electromagnetic transients on the European DEMO divertor. Part 1: Vertical displacement event, Fusion Engineering and Design, 175 (2022) 112999.

[21] F. Villone, L. Barbato, S. Mastrostefano, and S, Ventre, Coupling of nonlinear axisymmetric plasma evolution with three-dimensional volumetric conductors, Plasma Phys. Control. Fusion, 55 (2013) 095008.

[22] F. Villone et al., Report on 3D Electromagnetic analysis of DEMO disruptions, EFDA_D_2MUNQ3.